Maneuvering Target Detection in Over-the-Horizon Radar by Using Adaptive Chirplet Transform and Subspace Clutter Rejection

Genyuan Wang and Xiang-Gen Xia
Dept of ECE
University of Delaware
Newark, DE 19716
{gwang,xxia}@ee.udel.edu

Benjamin T. Root and Victor C. Chen
Radar Division
Naval Research Laboratory
Washington, DC 20375
{benroot,vchen}@radar.nrl.navy.mil

Yimin Zhang and Moeness.G.Amin
Center for Advanced Communications
Villanova University
Villanova, PA 19085
{zhang,moeness}@ece.villanova.edu

Abstract **In over-the-horizon radar (OTHR) target detection, the signal to clutter ratio (SCR) is very low, typically from –50 dB to –60 dB. Furthermore, for maneuvering targets, such as aircrafts and missiles, Doppler frequencies of their radar return signals may be time-varying. In this case, the Fourier transform based techniques and super resolution spectrum estimation techniques may not work well since they use sinusoidal signal models. In this paper, we propose a signal subspace clutter rejection algorithm combined with an adaptive chirplet transform technique for maneuvering target detection with OTHR. Simulation results by adding simulated maneuvering targets into raw OTHR clutter data are presented to illustrate the effectiveness of the proposed algorithm. The simulation results show that moving targets with –53.5 dB SCR can be detected.**

1. INTRODUCTION

Over-the-horizon radar (OTHR) has been widely used in detection and tracking of aircraft targets and ship targets in very wide-area surveillance, see for example [1-4]. The existing OTHR algorithms are based on the assumption that the Doppler frequency of target is constant during each dwell. A two-dimensional Fourier transform is taken to the received signal. Targets are detected from amplitude peaks away from the zero frequency. The detection capability of an algorithm depends on the SCR and the Doppler resolution. For a maneuvering target, such as an aircraft and a fast boat, the Fourier transformation based techniques may not work well due to the time-varying Doppler frequency nature of the signal. In this paper, we first propose an adaptive chirplet transform (ACT) for Doppler processing as an alternative of the Fourier transform, where the sinusoidal signal model is replaced by the chirplet signal model because the radar return signals from maneuvering targets have chirp type characteristics. With the ACT technique, the coherent integration time (CIT) can be extended, and therefore, the Doppler resolution may be better than that using the Fourier transform techniques. Since the SCR is very low, about –50 dB to –60 dB, before implementing the ACT, clutter reject algorithms must be used to improve the SCR. Most existing clutter rejection methods are integrated in signal spectrum estimation methods in target detection [3,9] for sinusoidal signal models, i.e., uniformly moving targets. Because the clutter in neighboring range cells have high correlation, the received signals from neighboring range cells are used to estimate the clutter covariance matrix, clutter subspace and signal subspace of the current range cell. When the signal subspace is accurately estimated, most clutter energy can be removed and the signal arrival from a target is kept after projecting the received signal into the signal subspace. We call this as *subspace clutter rejection algorithm* (SCRA) for convenience. The ACT is then applied to the clutter-removed signal, with which the maneuvering target signal energy can be focused. By using combined ACT and SCRA, our simulation results show that maneuvering targets with SCR at –53.5dB can be correctly detected. In this paper, we also consider the multi-path propagation environment that causes several received signals from each target to be possibly in different range, azimuth and Doppler cells. This may make the target detection and tracking more difficult. We show that our proposed algorithm is also helpful in multi-path signal detection because multi-path signals from a target with similar time-frequency distributions can be easily identified.

2. OTHR SIGNAL MODEL AND PROBLEM DESCRIPTION

In this section, we first describe the OTHR signal model presented in [4], the conventional OTHR processing for uniform moving targets, and then the problem of interest in this paper for maneuvering targets.

2.1 OTHR Signal Model for OTHR Processing

After the low pass filtering and sampling in the time interval, the received signal $s(n,m)$ for a target p with ground range r is, see for example [4],

$$s(m,n)=\sum_{l=1}^{L} A_{p_l}\exp\{j[\omega_{p_l} mT_c+(\omega_{p_l}-2\pi Bf(\frac{d_{p_l}}{c}-T_0))nT_s]\}+\xi_{n,m} \tag{1}$$

where n, m, T_0, ω_{p_l}, $\xi_{n,m}$ are the fast time sample index, chirp pulse index, the minimum delay, Doppler frequency shift, and additive noise, respectively. From (1), we find that the signal part in $s(m,n)$ in terms of index n is a complex sinusoidal signal. It is also a sinusoidal signal in terms of index m if the Doppler frequency ω_{p_l} does not change with m. In this case, a two-dimensional discrete Fourier transform over m and n provides the range-Doppler surface $S(m',n')$. For a particular OTHR processing algorithm, the target detection capability depends on the SCR. Therefore, in order to improve the target detection performance, one can increase the range, Doppler resolution, and the SCR. The range resolution, $\Delta r=\frac{c}{2B}$, depends on the radar system (the bandwidth B of radar), which is fixed for a fixed radar. However, the Doppler resolution, $\Delta\omega=\frac{2\pi}{T_c}$, depends on the CIT T_c, which is chosen at the receiver. Targets and clutter with a Doppler difference less than $\Delta\omega$ are located in one Doppler cell. One Doppler cell will be divided into k smaller cells and the SCR is then increased by k times if the CIT increases k times. The assumption here is that the target moves uniformly

within the CIT interval, which may not hold when the CIT is long.

2.2 Problem Description on Maneuvering Target Detection

For a maneuvering target, the signal Doppler frequency ω_{p_l} in (1) due to the target motion is no longer constant but time varying. The non-uniform motion of electron density distributions in ionospheric media can also induce the signal Doppler frequency change [9,10]. Consider a moving target with velocity v and acceleration a in the direction of slant range. The Doppler frequency ω_p in (1) is $\omega_p(t) = \frac{\pi}{\lambda}(v + at)$. The Doppler spread length is $\Delta\omega_p = \frac{\pi}{\lambda} aT_c$, and therefore, the number of Doppler cells that the target energy spreads over is $\frac{\Delta\omega_p}{\Delta\omega} = \frac{aT_c^2}{2\lambda}$. So, when the target moves uniformly, i.e., $a = 0$, the target energy using the Fourier transform is always concentrated in a single Doppler cell. It is, however, different when the target moves non-uniformly, i.e., $a \neq 0$. As an example, let us assume $a/(2\lambda) = 1$. In this case, the target energy spreads over T_c^2 Doppler cells. This implies that, if the CIT T_c increases k times, the number of Doppler cells over which the target energy spreads increases k^2 times. Therefore, in this case, the SCR in Doppler reduces k^2 times compared to that in the uniform moving target case. This tells us that, for a maneuvering target, the CIT increase does not benefit the OTHR target detection if the Fourier transform based technique is used in the Doppler processing. We next propose an adaptive chirplet transform (ACT) in the Doppler processing that takes advantage of the long CIT no matter whether the target moves uniformly or not.

3. CHIRP SIGNAL DETECTION AND ADAPTIVE CHIRPLET TRANSFORM

In OTHR, the received signal in a range cell is usually a multi-component signal with time-varying frequency since there may be multiple targets and clutter with different velocities in a range cell. If the CIT is not short, the received signal from a maneuvering target may be a linear chirp or a higher order time-varying frequency signal, i.e., a high order chirp. The idea in what follows is quite simple, i.e., a high order chirp from a target is expressed as a combination of several linear chirps over different time intervals called chirplets introduced by Mann and Haykin [8]. To a received signal $s(t)$, based on a given frame $\{h_k(t), k \in Z\}$, it will be decomposed as

$$s(t) = \sum_{i=1}^{N_0} \sum_k C_{i,k} h_k(t) u_i(t) \tag{2}$$

where $C_{i,k} = \langle s(t), h_k'(t) u_i(t) \rangle$ are the frame decomposition coefficients and $\{h_k'(t), k \in Z\}$ is dual frame of $\{h_k(t), k \in Z\}$, $\langle \bullet, \bullet \rangle$ represents the inner product and $u_i(t) = \exp\left\{ j(\frac{1}{2}\alpha_i t^2) \right\}$ for some chirp rate α_i. For details about (2), see [7,11]. To have an efficient frame decomposition, $\{h_k(t), k \in Z\}$ should include functions with different time and frequency widths and center (mean) locations. For example, the following modulated Gaussian functions

$$h_k(t) = \left(\frac{\gamma_k}{\pi} \right)^{1/4} \exp\left\{ -\gamma_k (t - t_k)^2 + j\left[\phi_k + \frac{\beta_k}{2}(t - t_k) \right] \right\} \tag{3}$$

are commonly used, where there are basically four indexes γ_k, ϕ_k, β_k, and t_k corresponding to the envelope, phase, frequency and time centers, respectively.

We next present how the chirp rate parameters α_i in $u_i(t) = \exp\left\{ j(\frac{1}{2}\alpha_i t^2) \right\}$ and the corresponding $h_k(t)$ of the form (3) are estimated. For a given signal $s(t)$, chirp rate α_1 is obtained by searching the largest peak in the Radon-Wigner plane after taking the Radon-Wigner Transform (RWT) of the signal $s(t)$. We then obtain frame $\{u_1(t)h_k(t), k \in Z\}$ by modulating frame $\{h_k(t), k \in Z\}$ in (3) with $u_1(t) = \exp(j\frac{\alpha_1}{2}t^2)$. We next estimate which element in the modified frame $\{u_1(t)h_k(t), k \in Z\}$ optimally matches the signal s and denote the element as $u_1 h_{k1}$ where

$$h_{k_1}(t) = \arg\min_k \left\{ \| s(t) - \frac{\langle s(t), u_1(t)h_k(t) \rangle}{\| h_k(t) \|} u_1(t) h_k(t) \| \right\}. \tag{4}$$

Define signal s_1 as

$$s_1(t) = s(t) - \frac{\langle s(t), u_1(t)h_{k_1}(t) \rangle}{\| h_k(t) \|} u_1(t) h_{k_1}(t). \tag{5}$$

By repeating the same procedure to $s_1(t)$ as to $s(t)$, we obtain the following things: parameter α_2 is obtained by estimate the largest chirp component of $s_1(t)$ by the RWT and let $u_2(t) = \exp(j\frac{\alpha_2}{2}t^2)$,

$$h_{k_2}(t) = \arg\min_k \left\{ \| s_1(t) - \frac{\langle s_1(t), u_2(t)h_k(t) \rangle u_2(t)h_k(t)}{\| h_k(t) \|} \| \right\}, \tag{6}$$

$$s_2(t) = s_1(t) - \frac{\langle s_1(t), u_2(t)h_{k_2}(t) \rangle}{\| h_k(t) \|} u_2(t) h_{k_2}(t). \tag{7}$$

Repeating the above procedure, signal $s(t)$ can be expressed as $s(t) = \sum_i s_i(t)$. Based on the above decomposition, the instantaneous frequencies of the signal's auto-terms can be obtained and then used for the OTHR target detection.

One can see that the search in (4) and (6) is in fact four dimensional, which has a high computational complexity. In order to reduce the complexity, a sub-optimal algorithm is given in [11] and summarized as follows:

Adaptive Chirplet Transform

Step 1. Estimate chirp rate α_1 and frequency ω_1 of $s(t)$ by RWT

$$(\alpha_1, \omega_1) = \arg\max_{(\alpha,\omega)} |D_s(\alpha, \omega)|.$$

Step 2. Generate $h_1(t)$ by a narrow band filter $g(t)$ with center frequency ω_1, $u_1 = \exp(j\frac{\alpha_1}{2}t^2)$ and $h_1(t) = g(t) \circ (s(t)u_1^*(t))$.

Step 3. The coefficient $C_{1,1}$ in (2) is obtained as follows

$$C_{1,1} = \langle s(t), h_1(t)u_1(t)\rangle = \int s(t)h_1^*(t)u_1^*(t)dt \ . \quad (8)$$

Step 4. Let $y_1(t) = C_{1,1}h_1(t)\ u_1(t)$, and $s_1(t) = s(t) - y_1(t)$. (9)

Step 5. Set $s(t) = s_1(t)$. .

Step 6. Stop if energy of $s(t)$ is small enough, otherwise go to Step 1.

4. CLUTTER REJECTION

As mentioned in the Introduction, the SCR is very low in the OTHR data. A clutter rejection algorithm is usually needed. The available clutter rejection algorithms [3,9] combine the adaptive clutter rejection and the maximum likelihood (ML) target detection together mainly based on the sinusoidal, uniformly moving target, signal model. These algorithms may not work well for maneuvering target detection because the target signals are chirps. In this section, we present a signal subspace clutter rejection algorithm that can remove large amount of clutter energy while keep the waveforms of moving target signals. After the clutter rejection, ACT is applied to detect maneuvering targets, characterized by chirps.

Signal subspace method is widely used in array signal processing and multi-user detection in wireless communications. In typical array signal processing, e.g., the MUSIC algorithm is applied, the signal to noise ratio is not too low. Signal subspace is estimated by the singular-value decomposition of the received signal covariance matrix. By using the estimated signal subspace and noise subspace a high resolution signal spectrum is obtained, which is used in targets detection. The difference between the OTHR application and the MUSIC is that the SCR is very low in OTHR and the desire signal frequency may be time varying. Therefore, a high resolution spectrum estimation may not achieve a good performance in OTHR target detection. Because the SCR in OTHR is very low (typically between –50dB and –60dB), it is impossible to directly estimate the signal subspace similar to array signal processing. However, signals from the neighboring range cells are highly correlated which can be used to estimate the clutter in an interested range cell. Let $s_c(t)$ be the received signal after range compression in the current interested range cell, $s_{n1}(t),...,s_{nN}(t)$ be received signals after range compression from N neighboring range cells. The covariance matrix of clutter and noise can be estimated by

$$R = \frac{1}{N}\sum_{i=1}^{N} s_{ni}s_{ni}^H \ . \quad (10)$$

The SVD decomposition of R can be written as $R = UVU^H$, where U is a unitary matrix and V is a diagonal matrix. Columns of U are eigen-vectors of R, and the elements in the diagonal of V are the corresponding eigenvalues. As the clutter is much stronger than noise and signal and is highly correlated between range cells whereas the signal has negligible correlation, the eigen-vectors $u_1, u_2, ..., u_M$ for some M corresponding to the largest eigenvalues are supposed coming from clutter. Therefore, the subspace $S_{clutter}$ generated from $u_1, u_2, ..., u_M$ is the clutter subspace. If the target signal is not in the subspace $S_{clutter}$, then $s_{proj}(t) = (I - P)s_c$, is the projection of received signal $s_c(t)$ in the current range cell into signal subspace, where

$$P = \sum_{i=1}^{M} u_{ni}u_{ni}^H \ , \quad (11)$$

is the projection operator to the clutter subspace $S_{clutter}$. Now the problem is how we can determine the number M of eigen-vectors $u_1, u_2, ..., u_M$ that belong to clutter subspace $S_{clutter}$. The signal $s_{\text{target}}(t)$ coming form a target may not be orthogonal to the clutter subspace $S_{clutter}$ if $u_1, u_2, ..., u_M$ are not appropriately chosen. In this case, the target signal $s_{\text{target}}(t)$ is also reduced or removed when clutter is reduced. We do not know the exact waveforms of targets. What we can do is to use the knowledge of estimated clutter covariance matrix to remove the clutter as much as possible while maintain the target signal as much as possible. Now, let us go back to (10), the estimated covariance R. Because only a few neighboring range cells are used to estimate R, it is rank deficient. Covariance matrix R_1 of clutter and noise can be estimated as $R_1 = R + \sigma^2 I$, where σ^2 is the variance of noise that is roughly known. R_1 has the following SVD decomposition and expression

$$R_1 = U_1V_1U_1^H = \sum_{i=1}^{N}\lambda_i\tilde{u}_i\tilde{u}_i^H = \sum_{i=1}^{N}\lambda_iP_i \quad (12)$$

where λ_i is the i-th largest eigenvalue of R_1, $\tilde{u}_i$ is its eigen-vector, and P_i is the projection operator to the subspace generated by $\tilde{u}_i$. From (12), one can see that the larger eigenvalues λ_i are, the more clutter energy distributes to the subspace generated by $\tilde{u}_i$. Based on this observation, the following algorithm is used to remove strong clutter without any knowledge of the signal

$$s_{proj}(t) = \sum_{i=1}^{N} f(\lambda_i)P_is_c(t) \ , \quad (13)$$

where $f(\lambda_i)$ is a decreasing function of λ_i. In (11), $f(\lambda_i)$ is

$$f(\lambda_i) = \begin{cases} 0 & i = 1,...M \\ 1 & i > M \end{cases} \ . \quad (14)$$

In our simulations of this paper, $f(\lambda_i)$ is chosen as $f(\lambda_i) = 1/\lambda_i$. In this case,

$$s_{proj}(t) = \sum_{i=1}^{N} f(\lambda_i)P_is_c(t) = \sum_{i=1}^{N}\frac{1}{\lambda_i}P_is_c(t) = R_1^{-1}s_c(t) \ , \quad (15)$$

which is obtained before applying the ACT. After this is obtained, the ACT is applied for the moving target detection.

5. SIMULATION

In this section, the performance of the proposed algorithms for maneuvering target detection is shown by some simulation results. The signal data coming from maneuvering targets is generated based on the signal model (1) and then added to the raw OTHR clutter data. The radar working frequency is 20MHz. There are 54 range cells in the data. Coherent integration time (CIT) is $T_c =$ 12.3 seconds. The velocity and acceleration of targets in the range direction are from $40\,m/s$ and 3 m/s^2, respectively. The signal to clutter ratio is about –53.5 dB.

In our simulations, the following steps are implemented. For the received signal, match filtering and range compression are first implemented in the range direction. Then, for each range cell, 6

neighboring range cells (3 range cells on each side) are used to estimate clutter covariance matrix of the current range cell. Next, the signal subspace clutter rejection algorithm is used to remove the clutter. After signal subspace clutter rejection, the ACT is used to the signal after the clutter rejection for target detection.

Fig.1 shows the signal waveforms before and after signal subspace clutter rejection of the range cell that contains a target. We can see that the clutter energy is suppressed by about 15 dB by using the signal subspace algorithm. Fig.2 depicts the range-Doppler results using the Fourier transform to data after the clutter rejection algorithms. Even the SCR is improved after the clutter rejection, the target remains undetectable, because the target energy is spread by using the Fourier transform to maneuvering targets. Instead of the Fourier transform in Fig.2, ACT is used in Fig.3. The target can be easily detected in Fig.3 at range 2250 km with Doppler frequency of about –4 Hz. The amplitudes of the signal in the range cell containing the target are shown in Fig.4, Fig.5 and Fig.6 using the Fourier transform without clutter rejection, the Fourier transform with clutter rejection, and the ACT with clutter rejection, respectively. From Fig.4, we can see that the clutter amplitude of the main lobe around 0 Hz is about 20 dB higher than that of the side lobes including the region around –5 Hz where the target is located. In Fig.5, although the clutter amplitude of the main lobe is reduced by about 15 dB and the side lode is reduced by about 5 to 10 dB, the target still can not be detected. But in Fig.6, the target energy is focused, and the amplitude of the target signal becomes about 4 dB higher than that of the clutter in target's neighboring frequency bands.

6. CONCLUSION

In this paper, an adaptive clutter rejection algorithm has been proposed to maneuvering targets detection in OTHR systems. This algorithm can reduce clutter energy by about 15 to 20 dB with negligible distortion to the waveform of the signal returned from maneuvering targets. An adaptive chirplet transform algorithm was applied to the clutter-mitigated signal for improved Doppler processing. Simulation results have shown that the proposed method substantially enhances the target detection ability. Particularly, several simulation examples have shown that the proposed method can successfully detect weak target signals where other methods fail.

REFERENCES

[1] G. D. McNeal, "The high-frequency environment at the ROTHR Amchitka radar site," *Radio Science*, vol.30, pp.739-746, May-June 1995.

[2] J. M. Headrick and J. F. Thomason, "Naval applications of high frequency over-the-horizon radar," *Nav. Eng. J.*, vol.108, pp.353-359, 1996.

[3] B. T. Root, "HF-over-the-horizon radar ship detection with short dwells using clutter cancellation," *Radio Science*, vol.33 no. 4, pp.1095-1111, 1998.

[4] R. Anderson and J. Krolik, "Target localization and track association for over-the -horizon radar with a statistical ionospheric model," *Technical Report*, Department of Electrical and Computer Engineering, Duke University, July 23, 1999.

[5] S. Qian, D. Chen, and Q. Yin, "Adaptive chirplet based signal approximation," *ICASSP'98*, Seattle, WA, 1998.

[6] V. C. Chen and W. J. Miceli, "Time-varying spectral analysis for radar imaging of maneuvering targets," *IEE Proceedings on Radar Sonar and Navigation*, vol. 145, Special Issue on radar Signal Processing, pp. 262-268, 1998.

[7] G. Wang and Z. Bao, "Inverse synthetic aperture radar imaging of maneuvering targets based on chirplet decomposition," *Optical Engineering*, vol. 39, no.9, pp. 1534-1541, 1999.

[8] S. Mann and S. Haykin, "The chirplet transform: physical considerations," *IEEE Trans. Signal Processing*, vol.43, pp.2745-2761, 1995.

[9] S. Kraut, K. Harmanci, and J. Krolik, "Space-time adaptive processing for over-the-horizon spread-Doppler clutter estimation," *Proceedings of ICASSP'2000*, pp. 3041-3044, 2000.

[10] L. J. Nickisch, "Non-uniform motion and extended media effects on the mutual coherence function: an analytic solution for spaced frequency, position, and time," *Radio Science*, vol.27, pp. 9-22, 1992.

[11] G. Wang, X.-G. Xia, B. T. Root, and V. C. Chen, "Moving target detection in over-the-horizon radar using adaptive chirplet transform," preprint, 2001.

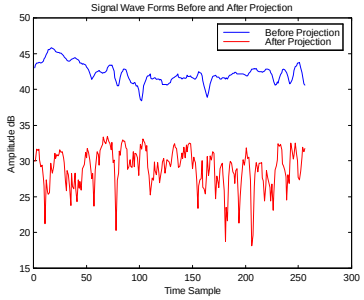

Fig.1

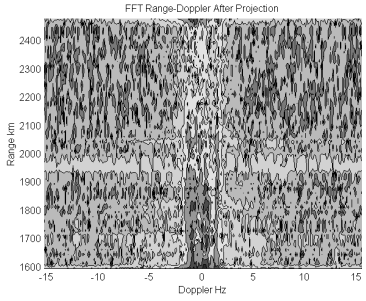

Fig.2

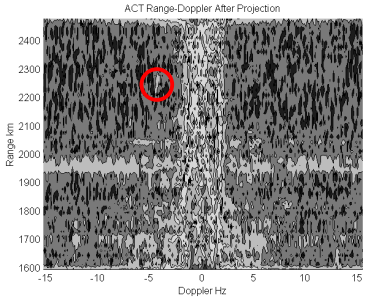

Fig.3

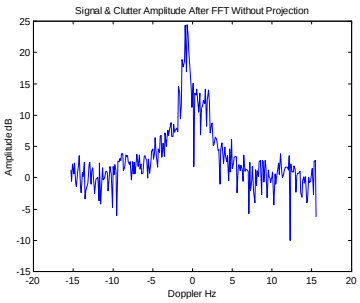

Fig.4

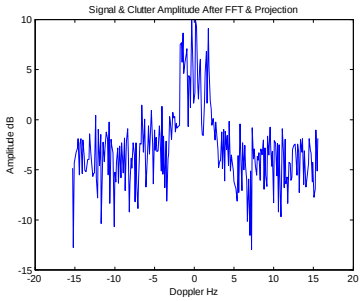

Fig.5

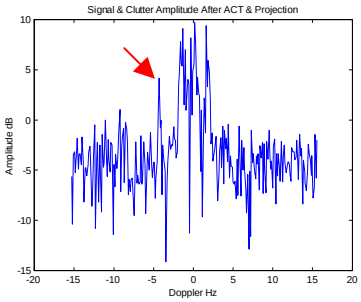

Fig.6